Thrombogenesis and Hemodynamics in Left Atrium Under Atrial Fibrillation

João Lameu[1], Italo Sandoval[1], João Salinet[1]

[1] Center for Engineering, Modeling and Applied Social Sciences (CECS), HEart Lab - Biomedical Engineering, Federal University of ABC (UFABC), São Bernardo do Campo, Brazil

Abstract

Atrial fibrillation (AF) is the most common sustained cardiac arrhythmia increasing the risk of stroke in five-fold. Improving knowledge at its development and prevention is crucial for AF patient management. This study aimed to predict the thrombogenesis in left atrium (LA) under AF by a multi-physics approach coupling a 3D transient profile of realistic electrophysiological activity, oscillatory mechanical effects and a biochemical model for thrombogenesis. The local mechanical effects from detailed AF activity disturbed the blood flow pattern, resulting in pro-thrombotic zones in left atrial appendage apex, in contrast with simplified AF model (rigid walls), that could lead to overestimation of pro-thrombotic zones.

1. Introduction

Atrial Fibrillation (AF) is the most common cardiac arrhythmia worldwide, being the main cause of cerebral ischemia, myocardium infarction and venous thromboembolism [1]. About one-third of arrhythmia related hospitalizations are due to AF. AF alters the contraction patterns of atria and could lead to increase in rigidity of atrial walls, consequently, leading to blood stagnation zones and pro-thrombotic environment, especially in the left atrial appendage (LAA) [2]. In healthy individuals, LAA presents high contractility, preventing blood stasis, in contrast with AF patients with reduced or absent LAA contractility [1].

Computational Fluid Dynamics (CFD) appears as a robust tool, allowing a multi-physics approach coupling electrophysiological and biomechanical aspects and also biochemical modeling of thrombogenesis. Numerical studies of AF considered rigid walls for left atrium (LA) as the worst scenario [3]. Few papers approached the mechanical effects of atrial walls, proposing idealized fibrillation patterns [3, 4] and reporting that more realistic patterns must be considered. Accordingly, this study aimed to predict the thrombogenesis in LA under AF through a multi-physical approach for electrophysiological, biomechanical and biochemical modeling of coagulation cascade.

2. Mathematical Modeling

The integrated model was developed in the CFD code Ansys Fluent (ANSYS, Inc.). AF electrophysiological activity was used as boundary condition for the hemodynamic simulations. Also, a simplified biochemical model was considered to evaluate the thrombogenesis risk.

2.1. AF Electrophysiological Activity

The electrophysiological activity was obtained from LA phantom by simulating a of rotor-type AF [5] using Python. The model (atrial shell) was composed by 284,578 nodes, with a gradient on the properties of it's cells, creating AF propagation patterns, as well as fibrotic tissue, modeled as nodes randomly disconnected [5, 6]. The activation frequency of the signals was firstly obtained by detecting the activation time with the wavelet method [6], then the frequency was calculated by the inverse of the time length between activation. The AF mapping was obtained for 64 points mimicking a multi-electrode array (Fig. 1-a). The AF frequency was re-mapped as a boundary condition in the CFD mesh (Fig. 1-b) to reproduce the local oscillatory mechanical effects into blood flow.

2.2. Governing Equations of Blood Motion

A transient model was proposed, considering incompressible blood (Carreau-Yasuda [9]) flow under laminar regime conditions [3, 4]. A patient-specific LA was taken from an opening dataset [10], being pre-processed in Ansys SpaceClaim (ANSYS, Inc.), and then a volumetric mesh with about 400,000 elements was created in Ansys Meshing (ANSYS, Inc.). The mass conservation and and momentum balance equations for the blood flow are given by Eq. 1:

$$\nabla \cdot \mathbf{U} = 0 \quad \text{and} \quad \rho \frac{D\mathbf{U}}{Dt} = -\nabla p + \nabla \cdot \tau + \mathbf{f} \qquad (1)$$

where ρ is the specific mass [ρ = 1055 kg m^{-3}], $\mathbf{U}$ is the velocity vector [m s^{-1}], p is the pressure [kg m^{-1}s^{-2}], τ is the viscous stress tensor [kg m^{-1}s^{-2}] and $\mathbf{f}$ represent the additional momentum source [kg m^{-2}s^{-2}] (Eq. 2).

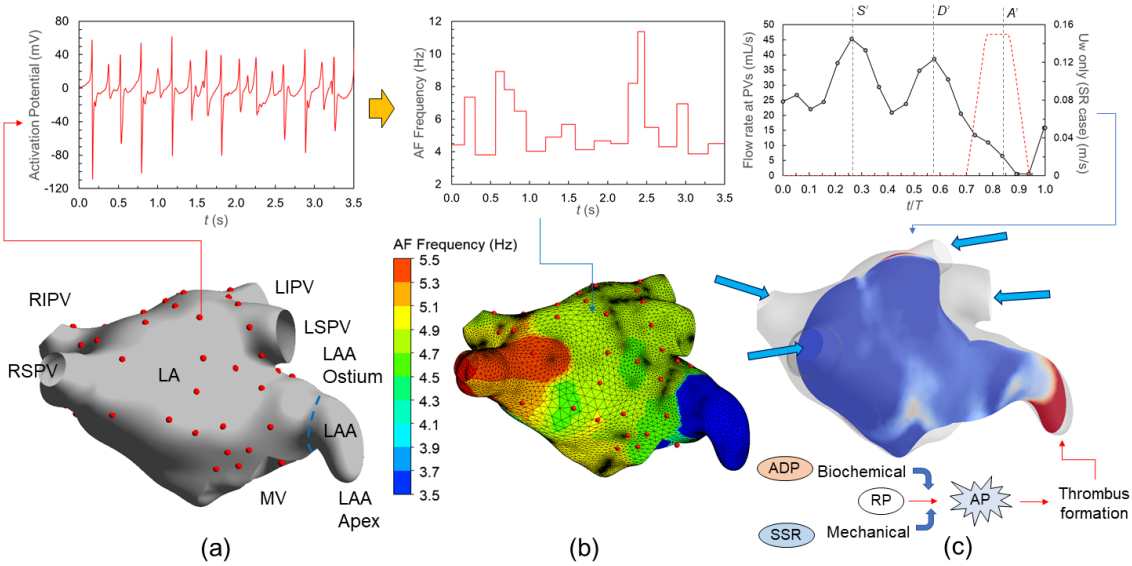

Figure 1. Schematics of AF electrophysiological data integration in the hemodynamic model: (a) 3D mapping of AF activity from 64-electrode with EGMs; (b) determination of local AF frequency (f_{AF}), providing a 3D transient map of f_{AF} as a boundary condition for the CFD to reproduce the mechanical effects of oscillatory wall motion; (c) definition of inlet flow rates (black line with dots) at pulmonary veins (PVs) [7], red dotted lines: LAA wall velocity, prescribed only for SR case [8], (d) coupling of biochemical model for thrombogenesis (T is the total cardiac flow cycle, LSPV - left superior pulmonary vein, LIPV - left inferior pulmonary vein, RSPV - right superior pulmonary vein, RIPV - right inferior pulmonary vein, LAA - left atrial appendage, AP - activated platelets, RP - resting platelets, ADP - adenosine diphosphate, SSR - shear strain rate).

2.3. Electromechanical Modeling

The mechanical effects of atria wall motion were considered by a momentum-based method, i.e., the atria walls were considered rigid and an additional source was included in the fluid momentum balance (**f** in Eq. 1). Basically, an inertial effect induced by the wall motion was considered (Eq. 2). The wall velocity (U_w) was considered to be an isotropic velocity field depending on the electrophysiological phenomenon. For SR case, the atrial contraction was based on a prescribed velocity function [8] at the end of the cardiac flow cycle (Fig. 1-c, red dotted lines). For AF case using realistic electrophysiological activity, the wall velocity was computed from the oscillatory wall displacement, d_w (Eq. 3), described by a first-order sinusoidal function, with wall displacement amplitude A = 0.88 mm (persistent AF) [11] and AF frequency given by the 3D transient profile (Fig. 1-b), ϕ is the electrophysiological activity coefficient, used to take into account the propagation effect of wall motion into blood flow.

$$\mathbf{f} = \rho\,\phi\left(\frac{U_w - \mathbf{U}}{\Delta t}\right) \tag{2}$$

$$U_w = \frac{d_w^{t_i} - d_w^{t_{i-1}}}{\Delta t} \quad \text{with} \quad d_w = A\,\text{sen}\,(2\pi f_{AF}\,t) \tag{3}$$

$$\frac{\partial \varphi}{\partial t} + \mathbf{U}\cdot\nabla\varphi = \phi_{activ} \tag{4}$$

where $\phi = \phi_{activ}$ = 1.0 for active walls, $\phi = \phi_{activ}$ = 0 for non-active walls, $\phi = \varphi$ for fluid domain.

2.4. Biochemical Modeling of Thrombogenesis

The simplified biochemical model for thrombogenesis (BMT) proposed by [12] was coupled to the hemodynamic model. The BMT starts from the intrinsic path of coagulation, that can induce thrombus generation in the absence of tissue factor. Two cellular species - resting (RP) and activated platelets (AP) and one biochemical species - adenosine diphosphate (ADP), were considered in the numerical model by advective-diffusive-reactive equations:

$$\frac{\partial [A_i]}{\partial t} + \mathbf{U}\cdot\nabla[A_i] = D_{A_1}\nabla^2[A_i] + S_{A_i} \tag{5}$$

where $[A_i]$ is the molar concentration of the i-th species (A_i = AP, RP, ADP) $[M]$, D is the mass diffusion coefficient $[m^2\ s^{-1}]$, S is the mass source due to the biochemical reactions $[M\ s^{-1}]$, given by two contributions: biochemical and mechanical, as detailed in [12].

2.5. Study Cases and Thrombus Indicators

Three study cases were performed with Carreau-Yasuda (CY) model: SR-CY: sinus rhythm, AF-CY: simplified AF case (rigid walls), AF-CY-3D-EGM: AF case with realistic 3D electrophysiological activity at LA walls. For the SR case, the cardiac flow cycle length was T = 940 ms (i.e. 64 bpm) [7], while for AF cases T = 462 ms (i.e. 130 bpm). 5 s of cardiac flow was simulated with time-step of $1 \cdot 10^{-3}$ s and a root mean square (RMS) residual of $1 \cdot 10^{-4}$. The inlet boundary condition was considered as the prescribed pulsatile flow (Fig. 1-c), considering flow rate symmetry among the PVs [2]. The outlet condition (mitral valve), was considered as a fixed open area with constant pressure of 8 mmHg [2]. The LA walls were considered rigid and the momentum-based method reproduced the oscillatory wall motion in AF cases, while a prescribed LAA wall velocity [8] was considered to reproduce the atrial contractility only for SR case. The boundary conditions for the BMT model were: [RP] = 10 $[nM]$, [AP] = 0.5 $[nM]$ (i.e., 5% of AP), [ADP] = 250 $[nM]$. Pro-thrombotic zones were estimated from wall shear stress indicators and thrombus aggregation intensity (ξ, Eq. 6). TAWSS is the time-averaged τ_w along the total cardiac cycle time T, OSI is the oscillatory shear index, ranging from 0 to 0.5 (0.5 indicates a strong recirculation zones) and RRT is the local relative residence time in $[\text{Pa}]^{-1}$. High OSI and RRT and low TAWSS indicate pro-thrombotic zones:

$$\frac{\partial \xi}{\partial t} = \alpha_\xi P_{\text{TSP}} \phi_f^2 - \beta_\xi \xi \tag{6}$$

where α_ξ and β_ξ are empirical constants for accumulation and destruction of thrombi [13], obtained from *in vitro* data in a Backward Facing Step (BFS) benchmark, P_{TSP} is the thrombus susceptibility potential, ranging from 0 to 1 as a function of WSS thresholds, ϕ_f is the fraction of activated platelets [13]. The stable thrombi generation is related to a ξ threshold. Since the BMT model employs accelerated kinetics, the threshold needed to be estimated considering the parameters from [12] and the proposed threshold (ξ_{BFS}) from [13]. Thus: $\xi_{threshold} \approx \xi_{BFS}(k_{kin,BQ} \cdot k_{kin,mech} \cdot t_{kin})/(k_{BFS,BQ} \cdot k_{BFS,mech} \cdot t_{BFS}) \approx 10^{-12} \cdot (10^8 \cdot 10^{-1} \cdot 10^1)/(1 \cdot 1 \cdot 10^3) \approx 10^{-7}[\text{cm}^{-3}]$, where the subscripts BQ and $mech$ denote for the magnitude of biochemical and mechanical kinetic constants, t is the timescale of stable clot formation, kin and BFS denotes for accelerated kinetics from [12] and data from [13].

3. Results and Discussion

Fig. 2 presents the time-averaged fields of WSS indicators (TAWSS, OSI, RRT) and instantaneous fields at the end of cardiac flow cycle (instant A', Fig. 1-c) for SSR, velocity and ξ after 4.5 s. From Fig. 2-a,b, it was observed low values of TAWSS (< 0.1 [Pa]) in the LAA under AF conditions. The AF-CY predicted stagnation zones in the whole LAA, with SSR < 10 s^{-1} (Fig. 2-e). The AF-CY-3D-EGM model predicted higher TAWSS, due to the local flow perturbation inherent from the oscillatory effect from AF activity. This mechanical effect propagates inwards the whole LA, including the LAA zone, where it was noticed higher TAWSS (Fig. 2-b) and SSR (Fig. 2-e), inherent from a slightly acceleration of blood flow (Fig. 2-f) regarding the AF-CY (rigid wall) model. The consideration of the atrial contraction by the momentum method in the SR model provided local acceleration of blood (Fig. 2-f) increasing the TAWSS (Fig. 2-a) and reducing the blood stagnation, as expected for healthy conditions. The OSI shows (Fig. 2-c) higher recirculation zones in the middle section of the LA (between left and right PVs) and also in LAA under AF conditions. The AF-CY-3D-EGM model predicted zones with higher OSI near to LAA ostium where the blood fluid accelerated (Fig. 2-f) due to the oscillatory perturbation from LA walls under AF. Consequently, larger RRT were observed in LAA (Fig 2-d) for AF cases. The results agree with the expected hemodynamics with stagnation zones inside the LAA under AF. Fig. 2-f shows the velocity fields at A' (atrial contraction), where it can be observed the local acceleration of the blood from LAA, reproducing its contractility under healthy conditions. This contractility (SR case), resulted in higher shear strain rates (Fig. 2-e) due to the local acceleration of blood, in contrast with the SSR < 10 s^{-1} in LAA from AF-condition, which is directly related to rouleaux formation and increment of blood apparent viscosity. The hemodynamic patterns directly affected the thrombogenesis prediction. Fig. 2-g shows the aggregation intensity field after 4.5 s. As expected from WSS-based indicators, higher values of ξ, above the $\xi_{threshold}$ were observed in the pro-thrombotic zone of LAA under AF conditions. The AF-CY model provided a larger zone above $\xi_{threshold}$ inherent from the strong stagnation over the whole LAA, while the AF-CY-3D-EGM model resulted in prediction of thrombi growth only at LAA apex.

4. Conclusions

The proposed model (AF-CY-3D-EGM) considering the 3D transient AF activity, oscillatory motion and simplified thrombogenesis model allowed a detailed description of hemodynamic features and thrombus generation under a realistic AF scenario. Simplified modeling of AF (rigid walls) could lead to overestimation of pro-thrombotic zones, with very reduced TAWSS (< 0.1 [Pa]) and higher OSI and RRT throughout the LAA. The consideration of 3D AF activity resulted pro-thrombotic zones mostly in LAA apex, inherent from the slightly blood recirculation induced by the oscillatory effects from LA walls.

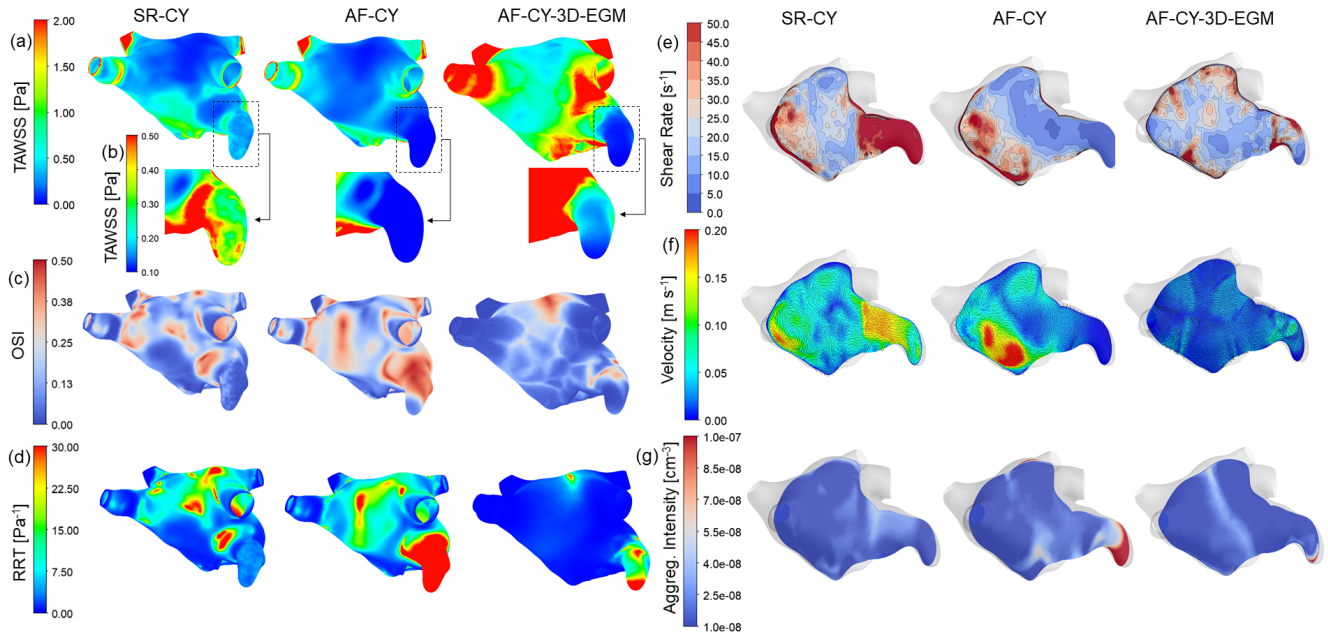

Figure 2. Numerical results from SR-CY, AF-CY and AF-CY-3D-EGM cases. (a)-(c) time-averaged fields at LA/LAA walls: (a) global TAWSS, (b) detail of TAWSS in LAA with reduced scale (between 0.1 to 0.5 [Pa]), (c) OSI, (d) RRT. (e)-(f) instantaneous fields at cross-sectional planes in LA/LAA at instant A': (e) SSR, (f) velocity. (g) aggregation intensity field after 4.5 s.

Acknowledgments

J. Salinet is supported by grant no. 2018/25606-2, São Paulo Research foundation (FAPESP). I. Sandoval is supported by Coordenação de Aperfeiçoamento de Pessoal de Nível Superior - Brasil (CAPES).

References

[1] Duenas-Pamplona J. et al. A comprehensive comparison of various patient-specific CFD models of the left atrium for atrial fibrillation patients. Comput Biol Med 2021; 133:104423.

[2] Mill J. et al. Sensitivity analysis of in-silico fluid simulations to predict thrombus formation after left atrial appendage occlusion. Mathematics 2021;9, 2304.

[3] Masci A. et al. The impact of left atrium appendage morphology on stroke risk assessment in atrial fibrillation: A computational fluid dynamics study. Front Physiol 2019;9, 1–11.

[4] Koizumi R. et al. Numerical analysis of hemodynamic changes in the left atrium due to atrial fibrillation. J Biomech 2015;48, 472–478.

[5] Rodrigo M. et al. Technical considerations on phase mapping for identification of atrial reentrant activity in direct- and inverse-computed electrograms. Circ Arrhythmia Elec 2017;10(9).

[6] Marques V.G. et al. A robust wavelet-based approach for dominant frequency analysis of atrial fibrillation in body surface signals. Physiol Meas 2020;41(7):075004.

[7] Fernandez-Perez G.C. et al. Analysis of left ventricular diastolic function using magnetic. Radiol 2012;4:295–305.

[8] Farese G.E. et al. Regional disparities of left atrial appendage wall contraction in patients with sinus rhythm and atrial fibrillation. J Am Soc Echocard 2019;32:755–762.

[9] Boyd J. et al. Analysis of the casson and carreau-yasuda non-newtonian blood models in steady and oscillatory flows using the lattice boltzmann method. Phys Fluids 2007; 19:093103.

[10] Roney C.H. et al. Predicting atrial fibrillation recurrence by combining population data and virtual cohorts of patient-specific left atrial models. Circ Arrhythm Electrophysiol 2022;15:e010253.

[11] Limantoro I. et al. Clinical correlates of echocardiographic tissue velocity imaging abnormalities of the left atrial wall during atrial fibrillation. Europace 2014;16:1546–1553.

[12] Grande-Gutiérrez N. et al. Computational modeling of blood component transport related to coronary artery thrombosis in kawasaki disease. Plos Comput Biol 2019; 17(9):E1009331.

[13] Taylor J.O. et al. Development of a computational model for macroscopic predictions of device-induced thrombosis. Biomech Model Mechanobiol 2016;15, 1713–1731.

João Lameu da Silva Jr.; Federal University of ABC (UFABC)
Alameda da Universidade, s/n, São Bernardo do Campo, Brazil
joao.lameu@ufabc.edu.br; https://heartlab.pesquisa.ufabc.edu.br